INSTITUTE OF PHYSICS PUBLISHING JOURNAL OF MICROMECHANICS AND MICROENGINEERING

J. Micromech. Microeng. **13** (2003) 1–7 PII: S0960-1317(03)37799-X

Design, realization and test of micro-mechanical resonators in thick-film silicon technology with postprocess electrode-to-resonator gap reducing

Dimitri Galayko[1], Andreas Kaiser[1], Lionel Buchaillot[1], Bernard Legrand[1], Dominique Collard[2] and Chantal Combi[3]

[1] IEMN-ISEN, UMR CNRS 8520, 41, bd Vauban 59046 Lille Cedex, France
[2] CIRMM/ISS-The University of Tokyo, Cite scientifique, Avenue Poincare, BP 69, 59652 Villeneuve d Ascq Cedex, France
[3] St Microelectronics, Via Tlolmeo, 1, 20010 Cornaredo, Milano, Italy

E-mail: dimitri.galayko@isen.fr and collard@isen.fr

Received 7 June 2003
Published DD MMM 2003
Online at stacks.iop.org/JMM/13/1

Abstract
This paper presents the design, fabrication and test of high-Q high-frequency lateral-mode clamped–clamped beam micro-resonators driven by parallel-plate electrostatic transducers fabricated in a thick epipoly technology. An innovative approach is employed to reduce an intrinsically high transducer gap value (>3.0 μm) required by the need of 15 μm thick structural layer etching down to 0.2–0.4 μm after the fabrication. This is achieved by employing an electrostatic motor that approaches the actuating and sensing electrodes close to the resonator. The electrode motor is driven with 30 V dc voltage, without any dc current consumption. Two resonators having a resonance frequency of 10 MHz have been fabricated with gap values of respectively 0.2 and 0.4 μm. A comparative analysis of performances of the two resonators is given in the paper.

1. Introduction

Since several years, MEMS technology seems to be an ultimate response to increasing demand of market for highly-integrated multi-standard RF mobile handsets. Three families of component are candidates for micro-mechanical implementation: RF switches (antenna switches), variable capacitances, RF and IF filters. Although promising results of microelectromechanical (MEM) filter design were demonstrated in numerous papers, a device suitable for commercial use in receivers is very difficult to realize. The existing works demonstrate a maximal center frequency of 158 MHz for a second-order filter (high-order filter working at frequencies of 300–400 MHz is required), use complex technologies for the device fabrication, and often require complex tuning to achieve a correct passband shape of high-order filters [1–5].

However, silicon-integrable inexpensive passive IF filters remain attractive components for mobile IF receivers, since their use allows us to reduce considerably the power consumption, the complexity of digital data processing. To get the (MEM) filters design and fabrication compatible with the industrial requirements, inexpensive fabrication technologies should be developed.

The main difficulty in the MEM filter fabrication is the achievement of a good-quality electro-mechanical transducers. Vibrating micro-mechanical system manufactured in silicon technologies usually employs capacitive transducers to transform voltage to force and mechanical displacement to charge variation.

Comb-drive transducers are commonly used for the excitation and sensing at low frequencies [3]. The advantage of the comb-drive transducers is their linearity, the disadvantages are large dimensions and mass which limit their use to low-frequency range (100–500 kHz). For high-frequency

MEM filters parallel-plate capacitive transducer is usually used [1, 2, 6]. Such transducers are easy to realize, they feauture small size and offer a much better flexibility of implantation for complex vibrating structures. The key point of realization of an efficient transducer is the implantation of a narrow gap between transducer's electrodes. In fact, the transduction factor, and so the power efficiency of the transducer, is inversely proportional to the second power of the gap width value. Thus for the case of simple resonator (elementary second-order bandpass filter) the motional resistance is inversely proportional to the fourth power of this parameter.

The motional resistance value intervenes in the input–output impedance adaptation, determines the insertion loss, and the output signal level. This resistance should be as low as possible. Practically, to achieve a resonator with a motional resistance value suitable for the use of the resonator in electronic signal-processing circuits, the gap value should be less than 0.2–0.5 μm, which is often below the lithography resolution of conventional MEMS fabrication processes.

So far, most of the realization of micro-mechanical resonators and filters was made by thin-film technologies [1, 2]. The employed methods of submicronic gap realization have been based on the definition of the gap by an oxide layer that was deposited on the resonator or on the electrodes, and then sacrificed. This approach requires complex and expensive technologies, hardly compatible with industrial environment.

In this paper we demonstrate a VHF 10 MHz micro-mechanical resonators fabricated in a thick-layer epipoly technology with an original post-fabrication gap reducing method. The fabrication technology is provided by ST Microelectronics, where it is commercialized and used for fabrication of low-frequency high-volume MEMS devices such as accelerometers. The technology uses one structural polysilicon layer 15 μm thick, where elements are patterned by dry etching. The minimum distance between two elements authorized by the lithography is 1.6–1.8 μm, and the overetching on the structural element edges is of 0.5–0.6 μm. Therefore, the minimally possible electrode-to-resonator gap value is about 3.0 μm. As shown by simulations and measurement results, VHF resonators with such a large gap have a too high motional resistance to achieve a good impedance matching, and so unusable for analogue filtering in electronic circuits.

2. Thick-film epitaxial polysilicon technology

The thick-film epitaxial polysilicon technology, called THELMA, was developed in ST Microelectronics for serial manufacturing of high-volume low-frequency devices (accelerometers). The availability of this technology in the industrial environment was one of the main reasons of using it for our work on micro-mechanical filters. Also, the high thickness of the structural layer offers several advantages for mechanical filter design. These advantages are (1) a strong stiffness along the vertical axis, which allows us to release large-area structures without sticking occurrence; (2) possibility to implement capacitive transducers with large electrode surface. The structure of a complete device fabricated in the technology is presented in figure 1.

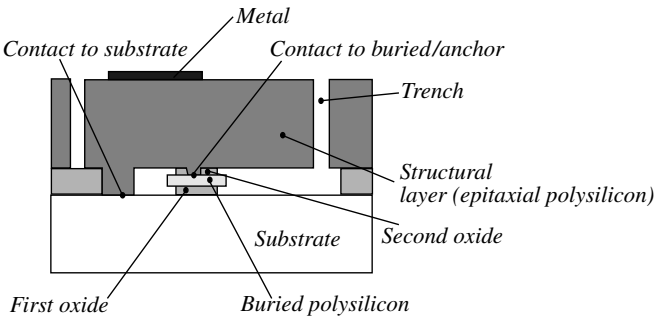

Figure 1. Structure of a device in THELMA technology.

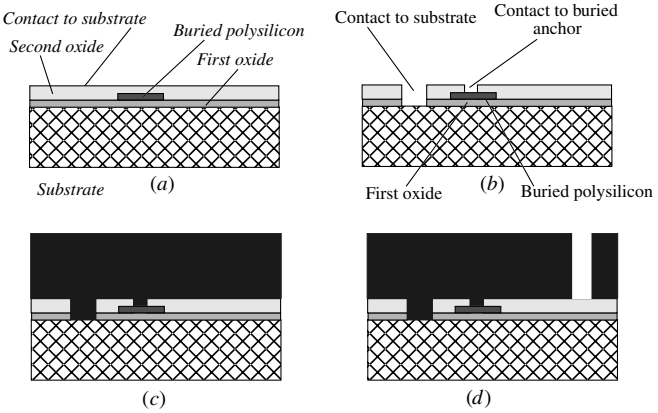

Figure 2. Fabrication of the device: (*a*) deposition of the first oxide, buried layer and sacrificial oxide; (*b*) definition of contacts to ground and to buried layer by sacrificial etching; (*c*) structural epitaxial polysilicon layer growth; (*d*) etching of the epitaxial layer.

The device is constituted of two polysilicon layers. One is the structural layer 15 μm thick, the second is a buried layer (0.45 μm thick), used for biasing. As shown in figure 1, these layers are separated by two oxide layers, and a contact is possible between the structural layer and buried layer and between the structural layer and the substrate. The manufacturing of the device is made in the following way. First an oxide layer is deposited on the substrate (2.5 μm thick) in a uniform way, then buried polysilicon is deposited and doped (0.45 μm thick). A sacrificial oxide is subsequently deposited (1.6 μm thick). These steps are shown in figure 2(*a*).

Then opening in the oxide layer is realized by sacrificial etching, defining future contacts to the substrate and to the buried layer (figure 2(*b*)).

The next steps are the epitaxial growth of the structural layer polysilicon (15 μm), its p-doping and a definition of trenches by dry anisotropic etching (figures 2(*c*) and (*d*)). The last step is a time-controlled removal of the sacrificial oxide 2 and the release. Thanks to a time-controlled releasing, the removed oxide width from trench edges is 3 μm (figure 3).

From the releasing method, it is clear that maximal width of a structure (or part) that can be released is 6 μm.

Trenches are realized by dry anisotropic etching. Because of the high thickness of the structural layer, only relatively large trenches can be achieved. The minimal authorized trench width defined on the mask level is 1.6 μm. Actual trench width is increased because of overetching. The overetching width is 0.5 $\pm$ 0.1 μm from each side, therefore the actual minimal achievable trench width is about 2.6 $\pm$ 0.2 μm. As stated in

Table 1. Thelma technology parameters.

	Structural layer	First oxide	Buried poly	Second oxide	Metal	Substrate
Thickness (μm)	15	2.5	0.45	1.6	0.7	–
Resistance	8 Ω/square	–	26 Ω/square	–	50 mΩ/square	1 Ω cm^{-1}

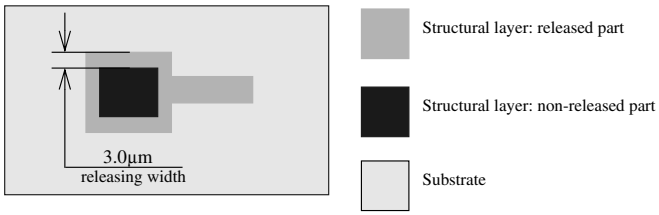

Figure 3. Demonstration of the releasing process: top view of device. The sacrificial oxide is removed only in vicinity of structural element edges.

the introduction, this value is too high to achieve an efficient capacitive transducer. The impossibility to realize narrow gap values constitutes the main disadvantage of the THELMA technology for micro-mechanical filter design. In the next section we will show how this difficulty is overcome.

To reduce the impedance of on-chip connection wires and to achieve a bonding, it is possible to deposit a Al/Si/Cu metal layer on the structural layer.

Table 1 summarizes the main parameters of the THELMA technology.

3. Post-fabrication gap reducing method

To reduce the electrode-to-resonator gap we propose to use an electrostatic motor that moves the input and output electrodes (sensing electrodes) close to the resonator. A schematic representation of one of the sensing electrodes with motor is shown in figure 4. The second one being identical. Figure 4(a) depicts the initially fabricated non-biased device state. The signal electrode is fixed to a rigid bar, which is suspended by a soft spring. The spring is anchored at the other end. The spring, the bar and the electrode are manufactured in the structural layer, and so electrically connected together. Near the rigid bar motor electrodes are placed. If they are biased regarding the sensing electrode (and so the rigid bar), an electrostatic field is created between the motor electrode and the bar, which generates a mechanical force acting on the bar. This mechanical force attracts it to the motor electrodes. If the force is sufficiently high, the spring deforms and the bar with the signal electrode fixed on it moves towards the motor electrode. The geometry of the device is designed in such a way that this displacement approaches the signal electrode to the resonator, and so the signal electrode-to-resonator gap reduces.

In order to limit the displacement and to avoid mechanical and electrical contact between the signal electrode and the motor electrodes or the resonator, stoppers are put near the bar (figure 4(a)). The distance from the stopper to the bar is less than the distance from the motor electrodes to the beam. After being approached, the rigid bar becomes clamped to the stoppers and remains in this state as long as the bias voltage on the motor electrodes is applied (figure 4(b)). The gap between the signal electrode and the resonator is reduced by the displacement value, which is equal to the initial (fabricated) distance between the sensing electrode and the stoppers. The stoppers are electrically isolated from the substrate and have a floating potential.

The device is biased in the following way: the resonator and motor electrodes are positively biased (these bias voltages are different in the general case), the signal electrodes are only connected to the signal source and to the output load, therefore the dc bias is zero.

If D_{res} is the initial (fabricated) signal electrode-to-resonator gap, D_{stop} is the initial (fabricated) distance from the signal electrode to the stoppers, the final signal electrode-to-resonator gap (D_{final}) is equal to $D_{\mathrm{final}} = D_{\mathrm{res}} - D_{\mathrm{stop}}$.

We note two advantages of the proposed method. First, on the initially fabricated, non-biased device any gaps between elements can be of values authorized by the lithography, greater than 3 μm, so the device dimensions are compatible with the lithography limitations of the THELMA technology. Since the actual signal electrode-to-resonator gap width is determined by the *difference* between the widths of two fabricated gaps, the actual signal electrode-to-resonator gap width can be very small, much smaller than initially fabricated ones. Secondly, the actual gap width does not depend on the overetching width of the structural layer. Since the actual gap value is defined by the difference between two fabricated gap values, the error due to overetching existing in each of them is cancelled, so the actual gap value is defined only by *designed* dimensions. This is very advantageous for the industrial use, because the overetching depends on numerous fabrication process parameters (etching method, etching time), and thanks to the differential nature of the gap value definition, these technological parameters are not required for the design.

4. Electrostatic motor design

It is obvious that the voltage applied to the motor should be as low as possible, in order to avoid the need of using high dc voltages in low-voltage electronic systems. This voltage depends on the spring stiffness, the initial (fabricated) distance between the motor electrodes and the signal electrode (V_{mot}), the surface of the active area of the motor electrodes, and the needed displacement value (the signal electrode-to-stopper distance D_{stop}). The equivalent mechanical scheme of the system is presented in figure 5(a). Depending on the relative position of the stoppers and motor electrodes with regard to the signal electrode, two cases are possible. (1) The final position of the signal electrode is located in the voltage-controlled position zone, where an equilibrium between the electrostatical force and the mechanical spring restoring force is possible, or (2) it is located in the pull-in zone, where such an equilibrium is not possible (for a fixed V_{mot}), and as soon as the voltage V_{mot} exceeds $V_{\mathrm{pull\text{-}in}}$, the signal electrode

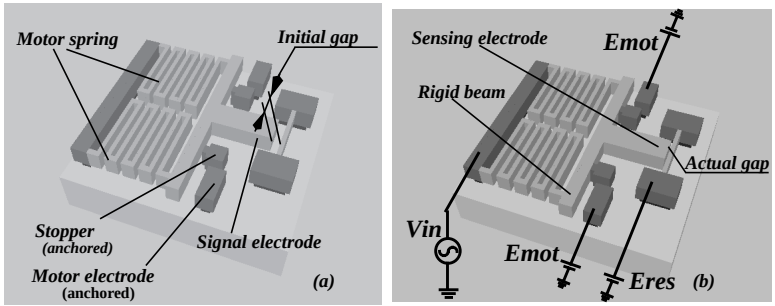

Figure 4. (a) The unbiased state of the resonator after fabrication; (b) the resonator with a biased motor: the sensing electrode is shifted close to resonator, the gap is reduced. Parts shown in dark are anchored, light parts are released.

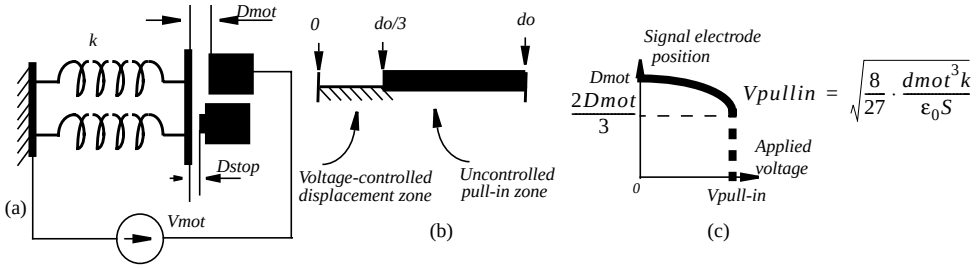

Figure 5. Motor operation: (a) equivalent mechanical scheme of the motor, (b), (c) demonstration of operating the system 'linear spring parallel plate capacitive transducer'.

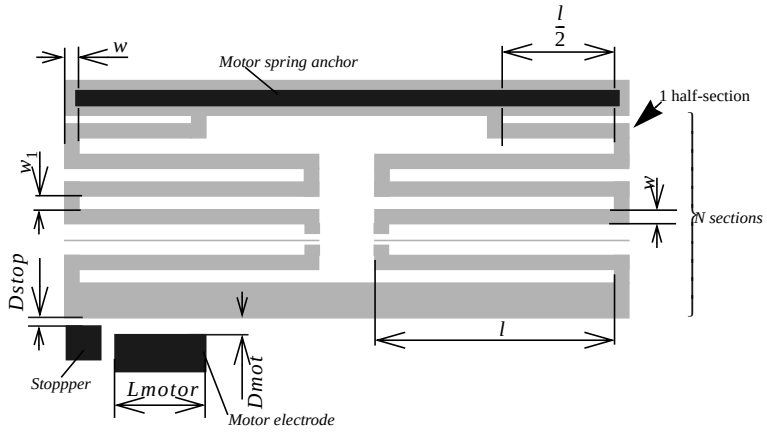

Figure 6. Motor spring dimension scheme.

moves towards the motor electrode until touching the stopper (figure 5(b)). The border between these zones is approximately located at the distance $D_{mot}/3$ from the initial position of the signal electrode, as shown in the plot of the figure5(c). To reduce the actuating voltage, the initial distance between the motor electrodes and the signal electrode (rigid bar) should be as small as possible. The lower limit is determined by the required displacement, i.e. by the distance between the stopper and the rigid bar. We have selected the latter to be 1.6 μm (at the mask level), equal to the minimum gap value allowed by the lithography. So the initial distance between the signal electrode (rigid bar) and the motor electrodes should be larger. We have chosen this gap to be 1.5 μm greater that the needed displacement. Thus, the initial distance from motor electrodes to the bar is equal to 3.1 μm (at the mask level). For an underetching width equal to 0.5 μm, the fabricated motor electrode-to-rigid bar distance is equal to 4.1 μm (3.1 + 2*0.5), the needed displacement 2.6 μm (1.6+2*0.5). It means that the final displacement point of the signal electrodes is located in pull-in zone, and therefore to activate the motor, at least the system's pull-in voltage should be applied (from figure 5).

To avoid deformations of the motor spring due to internal stresses of the structural layer, we designed the motor spring to be symmetrical and composed of two identical springs. Each spring is composed of eight long beams joined together in series, and one half-length beam. The geometry of the spring is shown in figure 6. The deformation of section beams produced by the displacement of the rigid bar in the axis x is quite complex, because the y-coordinate of the spring ends joined to the bar is fixed, i.e. this end is free sliding. Since sections are deformed differently, and have different end conditions, the analytical calculation of the stiffness of the overall spring is complicated. To determine the spring stiffness, we made a finite-element analysis with CoventorWare2001.3 software. For the dimensions indicated in table 2, the simulated spring stiffness

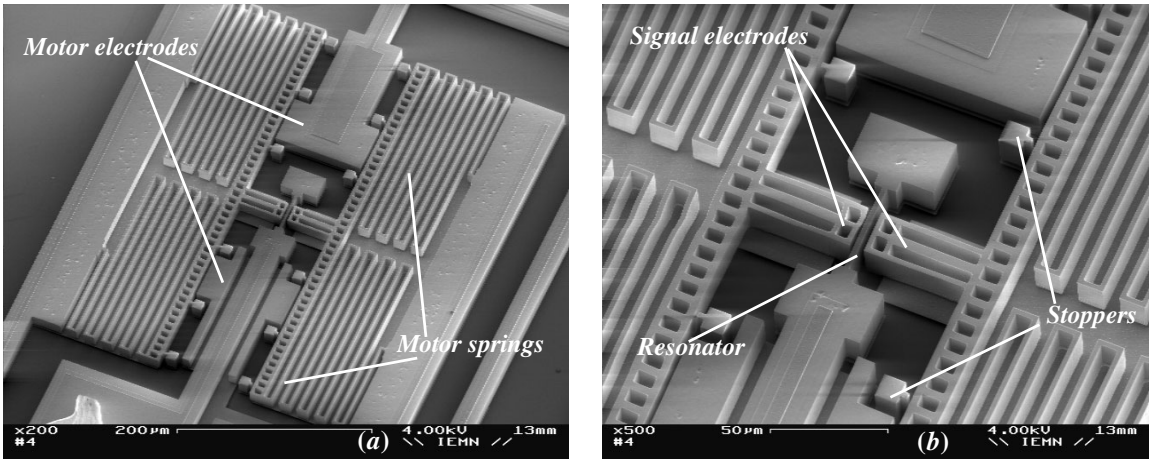

Figure 7. SEM pictures of the fabricated resonator in unbiased state (with actual gap 0.2 μm or 0.4 μm, the difference is too small to be visible on the picture).

Table 2. Basic motor and resonator's designed dimensions. Two values of D_{res} correspond to the two designed devices with different gaps, cf section 7. L_{motor} is the total length of the motor electrodes along the rigid beam.

Parameter	Value	Parameter	Value
l (μm)	197	D_{res} (μm)	1.8, 2.0
w (μm)	3	D_{stop} (μm)	1.6
w_1 (μm)	7	D_{mot} (μm)	3.1
N	8	Overetching width (μm)	0.6
L_{motor} (μm)	100	Resonator beam width (μm)	3
Resonator beam length (μm)	40		

value is equal to 0.32 N m^{-1}. Other geometrical configurations of the spring are possible.

If we assume that the stiffness of all beams are equal to those of unconstrained clamped-free beams, i.e. if we do not take into consideration the constraint imposed by the rigid bar, the calculated stiffness is equal to 0.1 N m^{-1}, three times less than the true value.

The dimensional parameters of the motor spring are given in table 2 (without consideration of overetching). To calculate the pull-in voltage of the system, we use the formula expressed for a linear-spring case (figure 5). It is possible because the displacements of the motor are very small compared to the spring dimensions, and so the spring can be considered linear. Using the simulated motor spring stiffness value and the motor electrode-to-rigid bar initial gap value, we obtain the pull-in voltage equal to 24 V.

5. Device fabrication

To demonstrate the validity of the proposed method of gap reducing, we fabricated two resonators with the same beam dimensions, with different initial gaps between the resonator and the signal electrodes, in the way to get the final gaps equal to 0.4 and 0.2 μm. All dimensions of the motor and resonators are given in table 2. Figure 7 shows SEM pictures with an overall view of the manufactured device and a close-up view of the resonator.

6. Motor test

The test of the motor has shown that the pull-in phenomenon occurs at $V_{\text{mot}} = 30$ V, close to the theoretically estimated value 24 V. After the gap is reduced, the motor bias voltage can be reduced to 15–20 V, and electrodes are still maintained close to the resonator. The motor does not consume any dc power. It should be noted that although the actual resonator-to-sensing electrode gap is unsensitive to the overetching, the actuating voltage is not. In fact, a different overetching width would yield a different beam width in the motor spring, as well as the distance between motor electrodes and the rigid beam. Thus, the actuating voltage can vary. We observed different actuating voltages for devices fabricated in different runs or being located at different points of the wafer (20–30 V).

7. Resonator test

We have especially been interested in characteristics that emphasize the signal electrodes-to-resonator gap reduction effects. For this the most informative is the resonance frequency shift versus bias voltage characteristic (figure 8). From this plot the real value of the gap can be extracted by curve-fitting [1]. The extracted gap values for the fabricated resonators are 0.27 μm and 0.57 μm, slightly larger than the designed values of 0.2 and 0.4 μm. The difference between the designed and the extracted gap values can be due to the fabrication mismatch: the overetching width can be slightly different for areas with different geometry, and 0.1 μm of tolerance is possible.

The resonance frequency of the resonator is found when the bias voltage tends to zero (no electrostatical spring exists). Although both resonators have been designed with the same dimensions, their resonance frequencies are different as we can see from figure 8 (9.98 MHz and 9.77 MHz). This is due to fabrication tolerances.

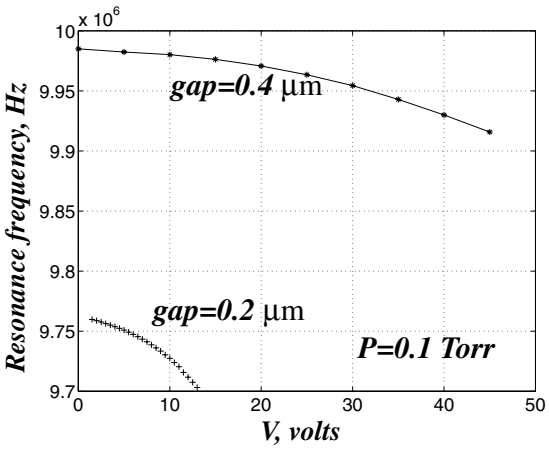

Figure 8. Resonance frequency versus bias voltage characteristics. The slope of the characteristic for the resonator with 0.2 μm gap is higher, as expected from theory [2]. The resonance frequency of the resonator corresponds to $V_b = 0$. The difference between the resonance frequency of identically designed resonators is due to fabrication errors.

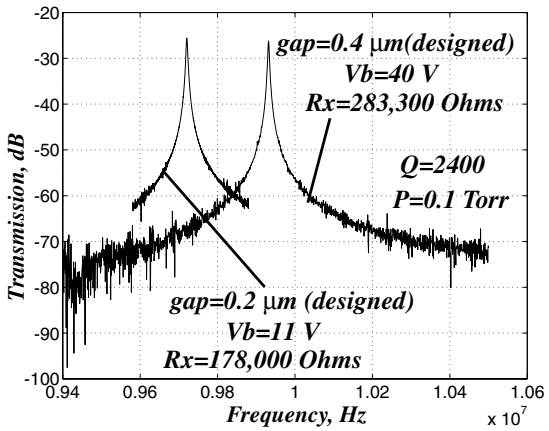

Figure 9. Comparison of the performance of two resonators. In spite of a ratio of 3.6 between the bias voltages, transmission levels are identical, which proves a better power efficiency of the resonator with smaller gap.

The following characteristic shows the influence of the gap value on the resonator performance. Two transmission characteristics have been measured for two resonators (figure 9). The bias voltages are chosen in order to get equal transmission at the resonance frequencies (and so an identical motional resistance). The ratio of the bias voltages of the resonators is $40/11 = 3.6$, close to 4, which proves that the ratio for the gaps is close to 2 $\left(R_x \sim \frac{d_0^4}{V_b^2}\right)$. To achieve the same transmission level without the gap reduction, the bias voltage would have to be close to 2500 V.

The values of motional resistances of two resonators mentioned in figure 9 have been obtained from the extracted gap values and simulated mechanical parameters of the resonators. They are not equal as expected from the equation of the transmission levels at the resonance frequency (37% difference). It can be explained by the inaccuracy of the extraction operation, since the motional resistance value is very sensitive to the extracted gap value $\left(\sim d_0^4\right)$, even small errors of the latter considerably affect the calculated value of the motional resistance.

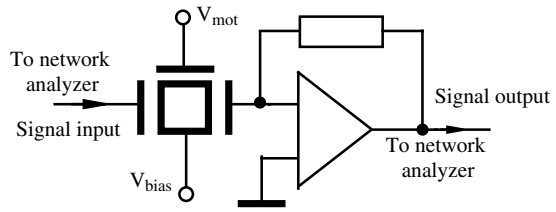

Figure 10. Resonator test set-up. A transresistance amplifier is used to achieve a low impedance in the input, and so to illiminate the influence of the parasitic parallel-to-ground capacitance at the output electrode of the resonator.

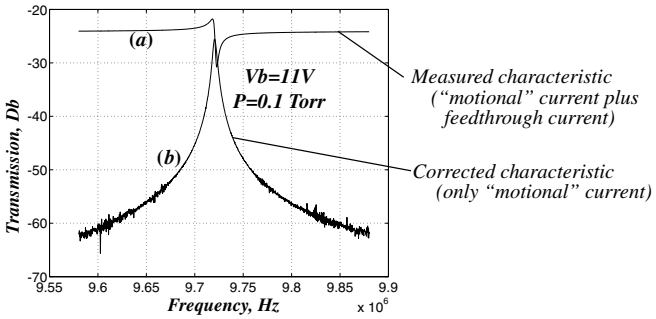

Figure 11. Demonstration of the parasitic coupling influence on the resonator characteristic.

8. Test set-up

To test the resonator performance, we have used the set-up shown in figure 10. This measurement scheme does not allow us to eliminate the parasitic capacitive coupling between the input and output electrodes from measurement results. This coupling creates a feedthrough current that is added to the motional current at the output. Since both signals are sinusoidal, their superposition gives a characteristic different from that of a single resonator (figure 11, plot a). To separate the motional resonator response from the parasitic coupling signal, we have adapted the method described in [7]. Using the set-up shown in figure 10, we first measure the resonator response with $V_b = 0$, i.e. only parasitic feedthrough current, and save the measured data in the network analyzer memory. We then measure the biased resonator response, and subtract the memorized data from the new measured signal containing both the feedthrough and the motional component. In this way an accurate measurement of the motional signal has been achieved (figure 11, plot b, and also plots in figure 9).

9. Conclusions

Test results have proved the effectiveness of the proposed method of the gap adjustment. It offers a possibility of designing micro-mechanical VHF filters in thick-layer silicon technology, where up to now the main difficulty was to achieve a sufficiently narrow gap without a complex technology. To drive the gap correction electrostatic motor, only 30 V dc without any current consumption is needed, which can be generated even in mobile systems. This issue contributes to the use of MEMS filters in commercial wireless applications. In this paper we have presented resonators with 10 MHz center frequency, but the method should allow the design of resonators and filters working at much higher frequencies

approaching the intermediate frequency band. Also, by appropriately modifying the geometrical parameters of the motor, the reduction of the motor actuating voltage is possible.

Acknowledgment

This work has been supported by the EU under contract number IST-1999-10945.

References

[1] Hsu W-T, Clark J R and Nguyen C T-C 2001 A sub-micron capacitive gap process for multiple-metal-electrode lateral micromechanical resonators *Proc. MEMS'01 (Jan. 2001)* pp 349–52

[2] Bannon F D III, Clark J R and Nguyen C T-C 2000 High frequency micromechanical filters *IEEE J. Solid-State Circuits* **35** 512–26

[3] Nguyen C T-C 1995 Micromechanical resonators for oscillators and filters *Proc. of the 1995 IEEE International Ultrasonics Symposium (Seattle, WA, 7–10 Nov. 1995)*

[4] Hsu W-T and Nguyen C T-C *Stiffness-Compensated Temperature-Insensitive Micromechanical Resonators: Proc. of MEMS2002 Conference (Las Vegas, NV)*

[5] Legtenberg R and Tilmans H A C 1994 Electrostatically driven vacuum-encapsulated polysilicon resonators, Parts 1 and 2 *Sensors Actuators* A **45** 57–84

[6] Tang W C, Nguyen T-C H and Howe R T 1989 laterally driven polysilicon resonant microstructures *Sensors Actuators* **20** 25–32

[7] Rantakari P, Kiihamäki J, Koskenvuori M, Lamminmäki T and Tittonen Reducing the effect of parasitic capacitance on MEMS measurements *Transducers'01, EUROSENSORS XV (June 2001)* Q1

[8] Galayko D, Kaiser A, Legrand B, Collard D, Buchaillot L and Combi C High-frequency high-Q micromechanical resonator in thick epipoly technology with post-process gap adjustment *Proc. MEMS2002* (USA: IEEE)

[9] Weigold J W, Juan W H and Pang S W 1998 Dry etching of deep SI trenchesz for released resonatours in a Cl2 plasma *J. Electrochem. Soc.* **145** 1767–71

[10] Howe R T, Boser B E and Pisano A P 1996 Polysilicon integrated microsystems: Technologies and application *Sensors Actuators* A **56** 167–77